

Nanotransfer printing by use of noncovalent surface forces: Applications to thin-film transistors that use single-walled carbon nanotube networks and semiconducting polymers

Seung-Hyun Hur and Dahl-Young Khang

Department of Materials Science and Engineering, University of Illinois at Urbana-Champaign, Urbana, Illinois 61801 and Beckman Institute and Frederick Seitz Materials Research Laboratory, University of Illinois at Urbana-Champaign, Urbana, Illinois 61801

Coskun Kocabas

Department of Physics, University of Illinois at Urbana-Champaign, Urbana, Illinois 61801 and Beckman Institute and Frederick Seitz Materials Research Laboratory, University of Illinois at Urbana-Champaign, Urbana, Illinois 61801

John A. Rogers^{a)}

Department of Materials Science and Engineering, and Department of Chemistry, University of Illinois at Urbana-Champaign, Urbana, Illinois 61801 and Beckman Institute and Frederick Seitz Materials Research Laboratory, University of Illinois at Urbana-Champaign, Urbana, Illinois 61801

(Received 30 July 2004; accepted 6 October 2004)

We report a purely additive nanotransfer printing process that uses noncovalent surface forces to guide the transfer of thin metal films from low-energy surfaces of high-resolution stamps to a variety of substrates. Structures with dimensions as small as a few hundred nanometers, with edge roughness as small as 10 nm are demonstrated. Metal multilayer stacks patterned in this way have electrical resistances that are the same as those formed by evaporation and conventional lithography. Thin-film transistors that use source/drain electrodes printed directly onto thin films of the semiconducting polymer regioregular polythiophene and networks of single-walled carbon nanotubes exhibit device mobilities and on/off ratios that are comparable to or higher than those of devices fabricated using standard methods. © 2004 American Institute of Physics.

[DOI: 10.1063/1.1829774]

Lithographic techniques based on molding,¹ printing,² and embossing³ are potential candidates for unusual applications in plastic electronics, biotechnology and other fields because they avoid many limitations of conventional methods. They also require only simple, low cost tools (i.e., molds, stamps, and presses). Several printing approaches have been recently demonstrated for patterning metal electrodes for organic electronic components (i.e., thin-film transistors, light emitting diodes, etc.); these include nanotransfer printing (nTP),^{4,5} soft contact lamination,^{6,7} cold welding,⁸ cathode transfer,⁹ and thermal imaging.¹⁰ The nTP method also has the ability to pattern three-dimensional and multilayer structures,⁵ which is a useful capability for other areas, such as nanophotonics and fluidics. In addition, when applied with soft, elastomeric stamps, nTP can be performed without the high pressures that are required with stamps made of rigid materials.^{8,9} In its current form, however, this technique is limited to systems in which specific covalent interactions guide the transfer of the solid inks from the surfaces of the stamps to the substrates. In this letter, we show that noncovalent surface forces can be sufficiently large to perform nTP. The flexibility that results from this general type of transfer expands considerably the range of materials and substrates that can be used. The implementation of metal multilayer stacks in this and the conventional form of nTP increases the mechanical integrity of the transferred films. We illustrate these ideas by fabricating classes of devices

that would be difficult to form by conventional nTP or other printing techniques: organic transistors that use source/drain electrodes formed directly on the top surfaces of thin semiconducting films of polymers and networks of single-walled carbon nanotubes (SWNTs).

Figure 1(a) schematically illustrates the steps for noncovalent nTP. Coating a stamp of poly(dimethylsiloxane) (PDMS) with a collimated flux of metal generates a discontinuous film on the raised and recessed regions. Placing this metal-coated stamp onto a flat, smooth substrate leads to “wetting” that provides intimate contact between the two surfaces without the need to apply external pressure. Mild heating (~50–80 °C) for sufficient time followed by removal of the stamp leaves a metal pattern in the geometry of the relief features on the substrate. Figure 1(b) shows an image of a PET substrate printed with a 30-nm-thick pattern of Au consisting of arrays of dots (diameters between 350 and 650 nm) in square lattices over an area of 0.5 × 0.5 cm. Figure 1(c) shows a SEM of one of these patterns. Figure 1(d) shows various device patterns printed onto a SiO₂/Si wafer; Fig. 1(e) shows optical and SEM images of a small area. These results illustrate uniform transfer over large areas (limited only by the size of the stamps) onto both polymer or inorganic substrates. The edge roughness of the features in both cases is ~10–30 nm. The transfer mechanism is based simply on the different strengths of nonspecific adhesion between the PDMS-metal and substrate-metal interfaces. In all cases described here, there is no known specific covalent chemical interaction between the materials used for printing and either the stamps or the substrates. The difference in

^{a)} Author to whom correspondence should be addressed; electronic mail: jrogers@uiuc.edu

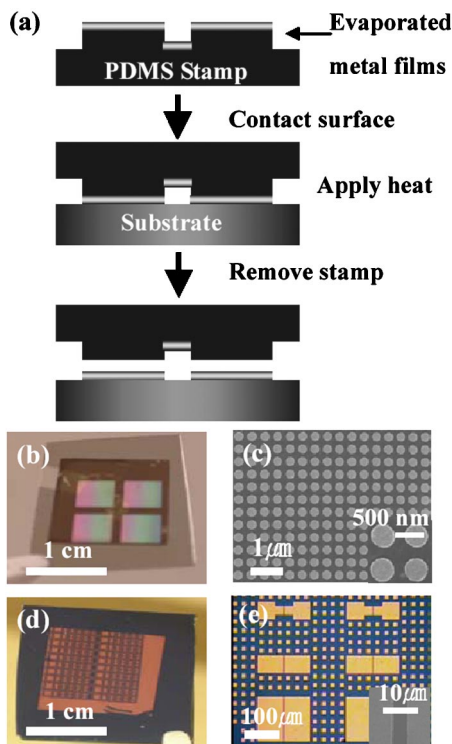


FIG. 1. (Color online) (a) Schematic illustration of steps for noncovalent transfer printing. Contacting a metal coated stamp to a substrate followed by moderate heating causes the metal to remain on the substrate after removing the stamp. (b) Optical micrograph of arrays of Au (30 nm thick) dots printed over an area of 0.5 cm \times 0.5 cm on a plastic substrate. (c) Scanning electron micrograph (SEM) of a small region of the printed pattern. (d) Optical micrograph of various Ti(2 nm)/Au(30 nm) device patterns printed onto a SiO₂/Si substrate. (e) Optical and scanning electron micrographs of a small region of the printed pattern.

work of adhesion of these two interfaces substrate-metal ($W_{\text{sub-metal}}$) and PDMS-metal ($W_{\text{PDMS-metal}}$), if we assume intimate material contact, can be written¹¹

$$W_{\text{sub-metal}} - W_{\text{PDMS-metal}} = (\gamma_{\text{sub}} - \gamma_{\text{PDMS}}) - (\gamma_{\text{sub-metal}} - \gamma_{\text{PDMS-metal}}), \quad (1)$$

where γ_{sub} and γ_{PDMS} are the surface energies of the substrate and the PDMS. The $\gamma_{\text{sub-metal}}$ and $\gamma_{\text{PDMS-metal}}$ are the interfacial energies between substrate and metal and between PDMS and metal, respectively.

The second term ($\gamma_{\text{sub-metal}} - \gamma_{\text{PDMS-metal}}$) can be much smaller than the first ($\gamma_{\text{sub}} - \gamma_{\text{PDMS}}$), since it is often the case that $\gamma_{\text{metal}} \gg \gamma_{\text{sub}}$ or γ_{PDMS} , where γ_{metal} is the surface energy of the metal. The difference in work of adhesion is then roughly equal to the difference in surface energies of the substrate and the PDMS. For most materials, the PDMS interface is weaker than the substrate interface, due primarily to the extremely low surface energy (19.8 mJ/m²) of the PDMS.¹¹ However, in the case of electron beam evaporated metal films, modifications in the surface of the PDMS can occur¹² which might increase the surface energy over the intrinsic value. We speculate that the heating step in the pattern transfer process of Fig. 1 facilitates diffusion of low molecular weight components of the PDMS to the stamp surface and/or reorientation and segmental motion of polymer chains in this region. Both effects accelerate surface hydrophobic recovery in the PDMS, which can weaken the interface by reducing $\gamma_{\text{PDMS-metal}}$.¹³ This heating may also im-

prove the contact between the surface of the metal film(s) and the substrate. Contact times of several days were necessary to transfer fully a layer of Au (30 nm) from PDMS to PET at room temperature but only ~ 2 h at 45 °C and ~ 30 min at 80 °C. The transfer was faster to a high surface energy substrate like PET (44.6 mJ/m²), polythiophene (38.0 mJ/m²), or polyimide (Kapton™; 37.4 mJ/m²) than to a low surface energy one like polypropylene (29.6 mJ/m²), poly[2-methoxy-5-(2'-ethylhexyloxy)-1,4-phenylenevinylene] (MEH-PPV) (28.0 mJ/m²) or pentacene (23.7 mJ/m²).¹¹ Transfer to an SiO₂/Si wafer with a monolayer of (tridecafluoro-1,1,2,2-tetrahydrooctyl)-trichlorosilane was much more inefficient than to a similar wafer without the monolayer. Exposing a stamp to an oxygen plasma to create a high-energy surface reduces dramatically the printing effectiveness compared to an untreated stamp. Depositing a thin (2 nm) layer of Ti (2.1 J/m²) on top of the Au increases the effectiveness of the printing compared to the bare Au (1.5 J/m²) case.¹⁴ The strength of adhesion of the Ti/Au film to the substrate was also greater than that of the bare Au film: the transferred patterns in the former case easily pass Scotch™ tape adhesion tests, whereas the ones in the latter case often do not. Transfer to substrates with large surface roughness was less effective than to those with small surface roughness. Collectively, these observations indicate that temperature, contact time, surface energy and substrate roughness are the main parameters that govern the noncovalent transfer process. We did not observe any significant variation of the transfer effectiveness with the size or geometry of the features of relief on the stamp.

To demonstrate the utility of noncovalent nTP in plastic electronics, we patterned source and drain electrodes directly onto a thin (25 nm) layer of the polymer semiconductor regioregular poly(3-hexylthiophene) (P3HT, Aldrich) deposited by spin casting onto a SiO₂(100 nm)/Si wafer from chlorobenzene and then baking for 5 min at 95 °C.¹⁵ The SiO₂ and Si provide the gate dielectric and gate, respectively. Figure 2(a) shows the drain current versus drain-source voltage at different gate-source voltages for a printed device whose channel length (L) and channel width (W) are 10 and 200 μm , respectively. Figure 2(b) compares the mobilities of devices with the same channel widths and lengths, but with electrodes of Au(10 nm)/Ti(5 nm)/Au(10 nm) patterned by printing and evaporation. The multilayer construction yields films with better structural integrity, higher conductivity, and fewer cracking defects than the case of Au alone. The shadow mask consisted of a thin sheet of polyimide machined with a high power laser to form channel lengths of 10, 20, 50, and 100 μm . The printed devices exhibit equivalent or slightly higher mobilities [Fig. 2(b)] than the evaporated ones; they also have 2–3 times higher on/off ratio, especially at small channel lengths. We believe that the degraded on/off in the shadow masked devices is due to metal that is not fully excluded from the channel region by the shadow mask. This effect, which derives from imperfect contact between the mask and the substrate, represents a practical challenge of shadow mask patterning at high resolution. The inset to Fig. 2(b) inset shows good scaling of saturation currents from printed devices with ratio W/L .

Noncovalent nTP can also form thin-film transistors that use networks of SWNTs as the semiconductor.^{16,17} The SWNTs substrates were prepared same as Ref. 17. Before

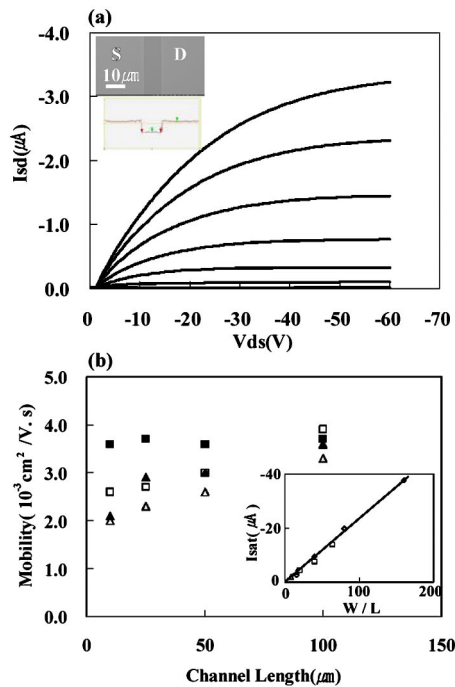


FIG. 2. (Color online) (a) Drain current (I_{ds}) vs drain-source voltage (V_{ds}) for a $200\ \mu\text{m}$ channel width and $10\ \mu\text{m}$ channel length P3HT organic film transistor whose electrodes were fabricated by transfer printing (gate voltage, V_{gs} : -60 to 60 V from the top, 20 V step). Top inset: Scanning electron micrograph (SEM) of the channel region. Middle inset: Atomic force micrograph of the channel region (x axis: $0\sim 50\ \mu\text{m}$, y axis: $-100\ \text{nm}\sim 100\ \text{nm}$). (b) Mobility comparison between transfer printed (solid) and evaporated (open) P3HT organic thin-film transistors in the saturation (square) and linear (triangle) regime as a function of channel length between 10 and $100\ \mu\text{m}$. Inset: saturation currents measured at a gate voltage of 60 V in ten different devices characterized by a wide range of channel widths and lengths.

breakdown, the effective thin film mobility of a typical device with W and L of 200 and $8\ \mu\text{m}$, respectively, was $30.7\ \text{cm}^2/\text{V s}$ ($15.4\ \text{cm}^2/\text{V s}$ device mobility) and its on/off ratio was 8 . Successive sweeps of V_{ds} from $0\sim -15$ V with the gate biased strongly positive caused gradual breakdown of the metallic pathways, along with an increase in on/off ratio. After sweeping 100 times in air the device showed a mobility of $1.7\ \text{cm}^2/\text{V s}$ ($0.85\ \text{cm}^2/\text{V s}$ device mobility) and on/off ratio of $\sim 10^3$. The behavior of these printed devices, which is shown in Fig. 3, was qualitatively similar to those formed by standard procedures.¹⁷

In summary, this letter introduces an operationally simple transfer printing technique that is capable of submicron resolution. The method does not rely on specific covalent interactions between the printed materials and the substrate, and in this sense it has significant flexibility in the materials that can be used. The use of multilayer stacks increases the mechanical integrity of printed metal films. The thickness, mechanical properties and surface roughness of the metal coatings as well as the roughness of the substrate must allow for the necessary intimate contact between stamp and substrate. The successful application of this method for patterning Au based electrodes for P3HT and SWNT transistors suggests that it might also be useful for building other devices such as light emitting diodes, solar cells and components in other areas.

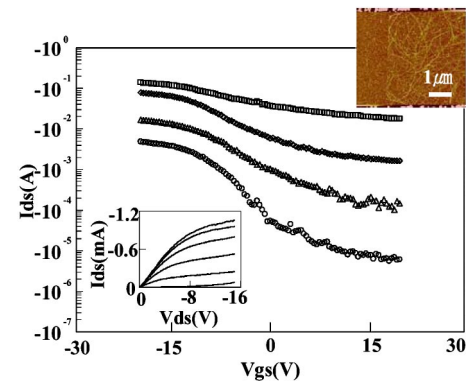


FIG. 3. (Color online) Transfer characteristics of SWNT network thin-film transistors before (\square -, $\mu=30.7\ \text{cm}^2/\text{V s}$, on/off ratio= 8) and after electrical breakdown of metallic pathways from source to drain electrodes. The breakdown was performed at $V_{gs}=20$ V, $V_{ds}=0\sim -15$ V sweep for 50 times (\diamond -, $\mu=25.8\ \text{cm}^2/\text{V s}$ on/off ratio= 49), 75 times (\triangle -, $\mu=5.2\ \text{cm}^2/\text{V s}$ on/off ratio= 166), 100 times (\circ -, $\mu=1.7\ \text{cm}^2/\text{V s}$ on/off ratio= 1014) in air. As we introduced parallel cuts by $5\ \mu\text{m}\times 5\ \mu\text{m}$ line and spacing, device mobilities are half of the thin-film mobilities. Top inset: atomic force microscopy image for SWNT device after making stripes and electrode (source and drain electrode are located on top and bottom). Bottom inset: Drain current (I_{ds}) vs drain-source voltage (V_{ds}) for a SWNT network transistor (W : $200\ \mu\text{m}$, L : $8\ \mu\text{m}$) measured after breakdown (V_{gs} : -20 V to 20 V from the top, 8 V step).

The authors thank T. Banks for help with the process and A. Shim of Dow Corning for helpful discussions. This work was supported by DARPA-funded AFRL-managed Macroelectronics Program (FA8650-04-C-7101). Funding is also partially provided by the U.S. Department of Energy under Grant No. DEFG02-91-ER45439. S.-H.H. and D.-Y.K. thank the Korea Science and Engineering Foundation (KOSEF) for the financial support.

- ¹E. Kim, Y. N. Xia, and G. M. Whitesides, *J. Am. Chem. Soc.* **118**, 5722 (1996).
- ²Y. Xia and G. M. Whitesides, *Angew. Chem., Int. Ed.* **37**, 550 (1998).
- ³S. Y. Chou, P. R. Krauss, and P. J. Renstrom, *Appl. Phys. Lett.* **67**, 3114 (1995).
- ⁴Y. L. Loo, R. L. Willett, K. W. Baldwin, and J. A. Rogers, *Appl. Phys. Lett.* **81**, 562 (2002).
- ⁵J. Zaumseil, M. A. Meitl, J. W. P. Hsu, B. R. Acharya, K. W. Baldwin, Y. L. Loo, and J. A. Rogers, *Nano Lett.* **3**, 1223 (2003).
- ⁶J. Zaumseil, K. W. Baldwin, and J. A. Rogers, *J. Appl. Phys.* **93**, 6117 (2003).
- ⁷T. W. Lee, J. Zaumseil, Z. Bao, J. W. P. Hsu, and J. A. Rogers, *Proc. Natl. Acad. Sci. U.S.A.* **101**, 429 (2004).
- ⁸C. Kim, P. E. Burrows, and S. R. Forrest, *Science* **288**, 831 (2000).
- ⁹J. Rhee and H. H. Lee, *Appl. Phys. Lett.* **81**, 4165 (2002).
- ¹⁰G. Blanchet, Y. L. Loo, J. A. Rogers, F. Gao, and C. R. Fincher, *Appl. Phys. Lett.* **82**, 463 (2003).
- ¹¹D. W. V. Krevelen, *Properties of Polymers* (Elsevier, Amsterdam, 1997).
- ¹²W. T. S. Huck, N. Bowden, P. Onck, T. Pardoen, J. W. Hutchison, and G. M. Whitesides, *Langmuir* **16**, 3497 (2000).
- ¹³B. T. Ginn and O. Steinbock, *Langmuir* **19**, 8117 (2003).
- ¹⁴L. Vitos, A. V. Ruban, H. L. Skriver, and J. Kollar, *Surf. Sci.* **411**, 186 (1998).
- ¹⁵Z. Bao, A. Dodabalapur, and A. J. Lovinger, *Appl. Phys. Lett.* **69**, 4108 (1996).
- ¹⁶E. S. Snow, J. P. Novak, P. M. Campbell, and D. Park, *Appl. Phys. Lett.* **82**, 2145 (2003).
- ¹⁷Y. Zhou, A. Gaur, S. Hur, C. Kocabas, M. A. Meitl, M. Shim, and J. A. Rogers, *Nano Lett.* **4**, 2031 (2004).